EFDA–JET–PR(08)38

V. Riccardo, G. Arnoux, P. Beaumont, S. Hacquin, J. Hobirk, D. Howell,
A. Huber, E. Joffrin, R. Koslowski, N. Lam, H. Leggate, E. Rachlew,
G. Sergienko, A. Stephen, T. Todd, M. Zerbini, R. Delogu, L. Grando,
D. Marcuzzi, S. Peruzzo, N. Pomaro, P. Sonato and JET EFDA contributors

Progress in Understanding Halo Current at JET

Progress in Understanding Halo Current at JET

V. Riccardo[1], G. Arnoux[1], P. Beaumont[1], S. Hacquin[2], J. Hobirk[3], D. Howell[1], A. Huber[4], E. Joffrin[1], R. Koslowski[4], N. Lam[1], H. Leggate[1], E. Rachlew[5], G. Sergienko[1], A. Stephen[1], T. Todd[1], M. Zerbini[1], R. Delogu[6], L. Grando[6], D. Marcuzzi[6], S. Peruzzo[6], N. Pomaro[6], P. Sonato[6] and JET EFDA contributors*

JET-EFDA, Culham Science Centre, OX14 3DB, Abingdon, UK

[1]EURATOM-UKAEA Fusion Association, Culham Science Centre, OX14 3DB, Abingdon, OXON, UK
[2]Association EURATOM-CEA, Cadarache, F-13108 St. Paul lez Durance, France
[3]Max-Planck-Institut für Plasmaphysik, EURATOM, D-85748 Garching, Germany
[4]Institute for Energy Research IEF-4, Forschungszentrum Jülich, Association Euratom-FZJ, Trilateral Euregio Cluster, Germany
[5]Euratom-VR Association, EES, KTH, Stockholm, Sweden
[6]Consorzio RFX –EURATOM/ENEA Ass., Corso Stati Uniti, Padova, Italy.
** See annex of F. Romanelli et al, "Overview of JET Results", (Proc. 22 [nd] IAEA Fusion Energy Conference, Geneva, Switzerland (2008)).*

Preprint of Paper to be submitted for publication in
Nuclear Fusion

ABSTRACT.
The poloidal distribution of the halo current density on the top dump plate in JET has been measured with a new set of Rogowskii coils. Although the interpretation of the measurements is still on-going, from the analysis so far it can be concluded that, during upward vertical displacement events, the measured current density is qualitatively consistent with the measured total poloidal current, the halo footprint extends over most of the upper dump plate and the observed halo current pattern is consistent with the measured heat flux.

1. INTRODUCTION

In the 2004-5 shutdown, 4 arrays of halo current diagnostics [1,2,3] have been installed behind the JET upper dump plate in octants 1 3 5 and 7 as part of the Halo Current Sensors (HCS) enhancement. Each array comprises 1 to 2 toroidal field (TF) pick up coils and up to 8 Rogowskii coils, one behind each tile of a poloidal row of tiles. In octants 1 and 7, the full complement of coils is not installed this is because of limitations in the in-vessel cabling at the feedthrough.

This set of sensors, complementary to refined measurement systems installed in other tokamaks [4-7], provides information on the dynamics of halo currents away from the divertor more detailed than that obtainable with the original TF pick-up coils (1 remaining at octant 3) and mushroom tiles (initially two per octant) [8] and the halo diagnostics installed behind the improved upper inner protection (IUIWP) in 2001 [9,10]. The IUIWP set comprises only 3 toroidal locations (octants 3 5 and 7), each equipped with just one large Rogowskii coil and one toroidal field pick up coil. The present layout of the halo current diagnostics in the top of the JET vessel is shown in Figure 1.

Initially all the HCS Rogowskii coils suffered from drifts, especially when Neutral Beam (NB) heating was applied and during disruptions. These drifts have been attributed to charge collection in the far scrape off layer. The problem has been addressed in the 2007 shutdown by installing protective covers in front of the in-vessel cabling. Figure 2 shows measurements from the same Rogowskii coil (octant 3 position 5, i.e. fifth row from the inboard) in a discharge before the 2007 shutdown (Pulse No: 70723) and in two discharges soon after (Pulse No's: 71346 and 71424). Before adding the cable covers, the signal did not come back to zero at the end of the pulse, when the background field returns to negligible values, suggesting the cause of the drift was not inductive. In particular the error was accumulated during the plasma phase and at a higher rate if NB power was applied. In addition, at the disruption the signal showed a step change which masked most of the tile collected current. Since the covers have been added, the signal now returns to ~zero and there is no drift during plasma or NB phases. The step at the disruption is greatly reduced, although changes difficult to reconcilable with magnetic pick-up might still occur occasionally.

While the signals from octant 3 are now ready for halo current mapping, those from octant 5 (the only other location with a large number of connected Rogowskii coils) appear still affected by cabling problems. Octant 1 and 7 have very few signals wired making them unsuitable for halo current density mapping, but still useful for consistency checks with the signals in octant 3.

2. INTERPRETATION

The Rogowskii coils are intended to measure the current collected by individual dump plate tiles.

The typical dimension of these tiles is a square of side 100mm. The expected current density is up to 300kA/m^2 in extreme events and up to ~100kA/m^2 in normal planned Vertical Displacement Events (VDE), which must be run at low plasma current to limit the vessel life consumption. Therefore the current routinely collected is ~1kA. Given the limited space envelope to fit a coil within a dump plate tile the cross section must be small (8.4mm times 5.4mm). In addition, to avoid problems terminating the wires a 0.65mm diameter mineral insulated cable was used; this allowed a relatively low packing density for the winding. The combination of small cross section and relatively low packing factor results in a low global coefficient ~1.8 10^{-7}Vs/A, which translates in to a low typical average signal of approximately 30mV, with an estimated peak of 100mV. Due to unavoidable inaccuracy in the winding process and additional small net areas of magnetic pick-up, the coil system (coil and in-vessel wiring) also suffers from unintended magnetic pick-up in its output voltage. In addition, the HCS was initially installed like all other magnetic systems in JET, i.e. with exposed braided cables between the in-vessel junction and the feedthrough. As discussed above the charge collection and leakage in the cabling also contributed to the signal, and in a substantial amount given the overall small contribution of the tile current. Once the drift caused by the charge collection in the cabling had been addressed, the magnetic pick-up has been removed following the usual magnetic compensation procedures. Magnetic pick-up typical of no-plasma and slow plasma transients is removed, with an error <200 A over the whole pulse.

As part of the process of validation of the observed dump plate tile currents, these have been compared with other halo current measurements in their neighbourhood, as shown in Figure 3. These comparisons show that the Rogowskii coil current timing is generally correct. However, the signal can grow before halo current is detected elsewhere, for example in the mushroom tiles, which being at a lower position should interact with the edge of the plasma before or at the same time as the dump plate, at least in weakly shaped disruptions. This feature probably has to be attributed to radial field pick-up beyond compensation, as this is optimised for steady state conditions. For example in a typical low triangularity disruption of a 2MA plasma up to 300A are measured before the plasma is believed to have become limited on the dump plate when the plasma has displaced ~0.3m, so an error of ~500 10^{-6} A/(Am); a slightly larger error appears in disruptions of high triangularity plasmas. This error is not removed in the following analysis.

In addition, the quality of the signals deteriorates after the thermal quench, more dramatically in disruptions of plasma with high energy content. This might be because the covers added in the 2007 shutdown are insufficient to screen high levels of charge fluxes.

The set of polarities used in the following analysis of the octant 3 measurements has been defined by testing different combinations on a large set of VDEs and vertical disruptions, and selecting the one that gives consistent results. For two rows (6 and 8) a sign that survived all the types of disruptions assessed could not be found. Therefore these two rows are not used: row 6 has been taken as the average of rows 5 and 7, while row 8 has been removed. Preliminary integral checks show that the measured halo current density is consistent with the poloidal halo current measured by the TF pick up coils. For example, the time average, between 65.011 and 65.021 s, of the net halo current collected on the dump plate in Pulse No: 74449 is 530kA, while the poloidal current measured at the inner TF pick up coil is 350kA.Taking into account that (a) the dump plate is uneven, so with

shallow field lines collection is enhanced where the tile misalignment is larger, such as at the edge of a plate, like the location of the Rogowskii coils, (b) the halo current is not necessarily toroidally uniform and (c) there might be an offset due to the enhanced magnetic pick-up beyond that removed by the steady state magnetic compensation, these two values are in relatively good agreement.

As part of the validation process the signal in octant 3 with signals from a corresponding tile from octant 1 and 7 have been compared. The signals in the 3 octants have overall similar behaviour, but sometime rather different on a finer time scale. Two features that recur in most comparisons are: (1) the amplitude of row 3 in octant 3 tends to be larger than in the other octants and the difference seems to be mainly linked to the magnetic pick-up during the plasma vertical displacement and (2) row 5 in octant 1 has systematically a larger step. Postprocessing of the measurements at the other octants is not yet routinely available.

3. RESULTS

In the following the poloidal map of halo current on the dump plate is discussed in some detail for three disruptions. These have been chosen as to represent a fairly wide range of disruption typologies.

First of all two planned ohmic disruptions are presented. The advantage of using ohmic events is that the Rogowskii coils are less affected by charge collection in the later stages and so steps in the measurements appear later. The two events chosen are a high triangularity "abrupt" VDE (Pulse No: 72914, shown in Figure 4) and a low triangularity "gentle" VDE (Pulse No:74449, shown in Figure 5). The type of VDE does not seem to affect the quality of the data, from this point of view the choice was guided by availability. An "abrupt" VDE is obtained by applying a large bias voltage to the radial field for 10 ms and then clamping the voltage to zero. A "gentle" VDE is obtained applying a smaller voltage for a shorter time and by letting the control system try to recover the plasma after the kick.

In the high triangularity event (72914), the position of the plasma contact region on the dump plate in the initial stages of the event (source centred at row 4 and sink in contact with row 1) is consistent with the EFIT reconstruction. Unfortunately, the last converging EFIT reconstruction is at 66.0165 s, as this code does not converge when current is flowing in open flux tubes. Following the (modest) thermal quench, the position of the outer region of plasma interaction with the dump plate moves from row 4 to row 7, while the inner region falls off the inner side of the dump plate completely. To validate this, plasma reconstruction robust to the flow of current in open flux tube would be advantageous, and is planned.

In the low triangularity event (Pulse No: 74449), the position of the plasma contact region on the dump plate remains constant through out, at least until some signal suffer from a step change. This behaviour is typical of the low triangularity events analysed. The last converging EFIT reconstruction is at 64.998 s, before the plasma becomes limited on the dump plate.

The last event, Pulse No: 73124, shown in Figure 6, is a high plasma stored energy planned low triangularity VDE. The disadvantage is that the quality of the signals is poor after the thermal quench. The advantage is that this offers the opportunity to compare halo current and heat load deposition patterns. The reason for the need for high plasma stored energy is not only because the heat loads are smaller on the dump plate otherwise, but also because there is an uncertainty in the

trigger time of the Infra-Red (IR) camera data collection, which can be significant on the disruption time scale. The absolute time is more easily recovered if ELMs are present and can be used to synchronise the IR data to the global pulse data. In order to have ELMs visible on the dump plate (having the IR collection region being cropped so as to allow faster data sampling, suitable for a disruption) the plasma had to be in a good H-mode before the vertical instability was initiated.

The halo current pattern on the dump plate during the initial stages of the Pulse No: 73124 VDE is similar to that of 74449, and in general to low triangularity events. The IR data collected in this event have been processed as described in detail in [11]: the 2D temperature of the dump plate contains features due to the geometrical layout, so it is simplified in to a toroidally average 1D poloidal temperature profile, which can be converted using THEODOR [12] in to a heat load profile. Figure 7 shows that both the halo current profile and the heal load profile peak between 200mm and 600mm. Even if the absolute peak is not at the same poloidal position, the agreement is remarkable for two such different and independent methods of observing plasma wall interaction.

The peak halo current density is consistent with expectation, even if slightly high for the predisruption plasma current. The design criteria applied for JET in-vessel components is 300kA/m^2 over a 1m poloidal arc for a 6MA disruption, while here ~160 kA/m^2 are found for a 2.25MA disruption. This could be partly due to part of the observed collected current being spurious magnetic pick up and partly due to the halo footprint extent being smaller than anticipated (but still large). If this behaviour is substantiated, consideration will have to be given to updating the standard assumptions used in stress analysis of proposed in-vessel assemblies.

In Pulse No: 73124 the bolometric diagnostic was set up so as to avoid saturation during the disruption. This allows tomographic reconstruction of the radiation during the disruption and, following a procedure described in more detail in [13], the estimate of radiation poloidal profiles on the plasma facing components. Figure 8 contains a set of tomographic reconstructions and the corresponding radiation poloidal profiles. The peak radiation moves from the outboard of the dump plate, in the region of the mushroom tiles, to the centre of the dump plate between the thermal quench and the peak of the total radiation (66.0395 s).This is consistent with the expected diamagnetic response of the plasma (inward jump) and the variation between preand post- thermal quench profiles observed by the IR. Further dump plate specific analysis including absolute power density will help the interpretation of the IR data.

SUMMARY AND CONCLUSIONS

In-vessel Rogowskii coils with adequate sensitivity and signal to noise for halo measurements are very challenging in the JET environment. Nevertheless detailed measurements of the distribution of the halo current have been possible, and the following conclusions can be drawn:

- The halo footprint extends over most of the dump plate during upward events.
- The measured current density is consistent with the measured total poloidal current.
- The observed halo currents flow through the same region of the dump plates as the heat flux measured by the IR camera at the thermal quench for upward VDEs.

The new data broadly confirms the extrapolations made on the halo measurements previously available at JET. Some features such the width of the halo region (from the measured footprint

extent) and the location of the halo-wall contact region during a disruption will benefit from equilibrium reconstruction able to deal with current flow along open field lines.

ACKNOWLEDGEMENTS

This work was funded jointly by the UK Engineering and Physical Sciences Research Council and by the European Communities under the contract of Association between EURATOM and UKAEA. It was carried out within the framework of the European Fusion Development Agreement. The views and opinions expressed herein do not necessarily reflect those of the European Commission.

REFERENCES

[1]. Pomaro N. et al., Rev. Scient. Instr., **74** (2003) 1567-1570
[2]. Sonato P. et al., Fus. Eng. Design, **74** (2005) 757-761
[3]. Peruzzo S. et al., Fus. Eng. Design, **82** (2007) 1287-1293
[4]. Pautasso G. et al., 28th EPS, Madeira (2001) P-1.005
[5]. Neyetani Y., Characteristics of halo currents in JT-60U, Nucl. Fusion **39** (1999) p.559
[6]. Evans T. et al., J. Nucl. Mater. **241–243** (1997) p.606
[7]. Counsell G. et al., Plasma Phys. Control. Fusion, **49** (2007) 435-446
[8]. Andrew P. et al., Proc. 16th SOFE (1995)
[9]. Riccardo V. et al., Fus. Eng. Design, **66-68** (2003) 1567-1570
[10]. Riccardo V. et al., Plasma Phys. Contol. Fusion, **46** (2004) 925-934
[11]. G Arnoux G. et al., EX/7-2Ra, Proc. 22nd IAEA Fusion Energy Conference, Geneva, 2008
[12]. Herrmann A. et al., Plasma Phys. Control. Fusion, **37** (1995) 17-29
[13]. Huber A. et al., " Plasma Radiation Distribution and Radiation Loads onto the Vessel During Transient Events in JET", to be published in Journ. Nucl. Mat.

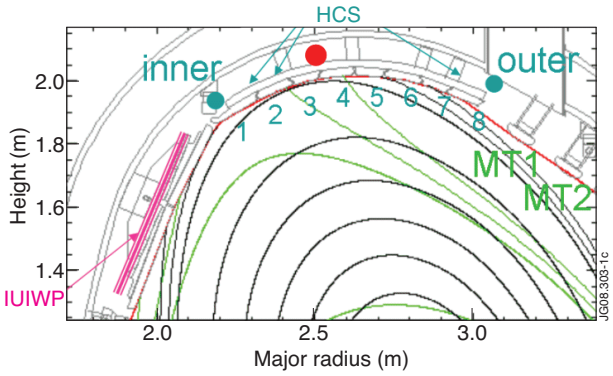

Figure 1: Schematic summarising the layout of the halo current diagnostics in the top of the JET vessel. (1992): one TF pick-up coil behind the centre of the dump plate (oct 3) and two mushroom tiles (MT1 and MT2) shunts. (2001) IUIWP: one TF pick-up coil and one large Rogowskii coil (oct. 3, 5, 7). (2004) HCS: ≤2 TF pick-up coils and ≤8 Rogowskii coils (oct 1, 3, 5, 7).

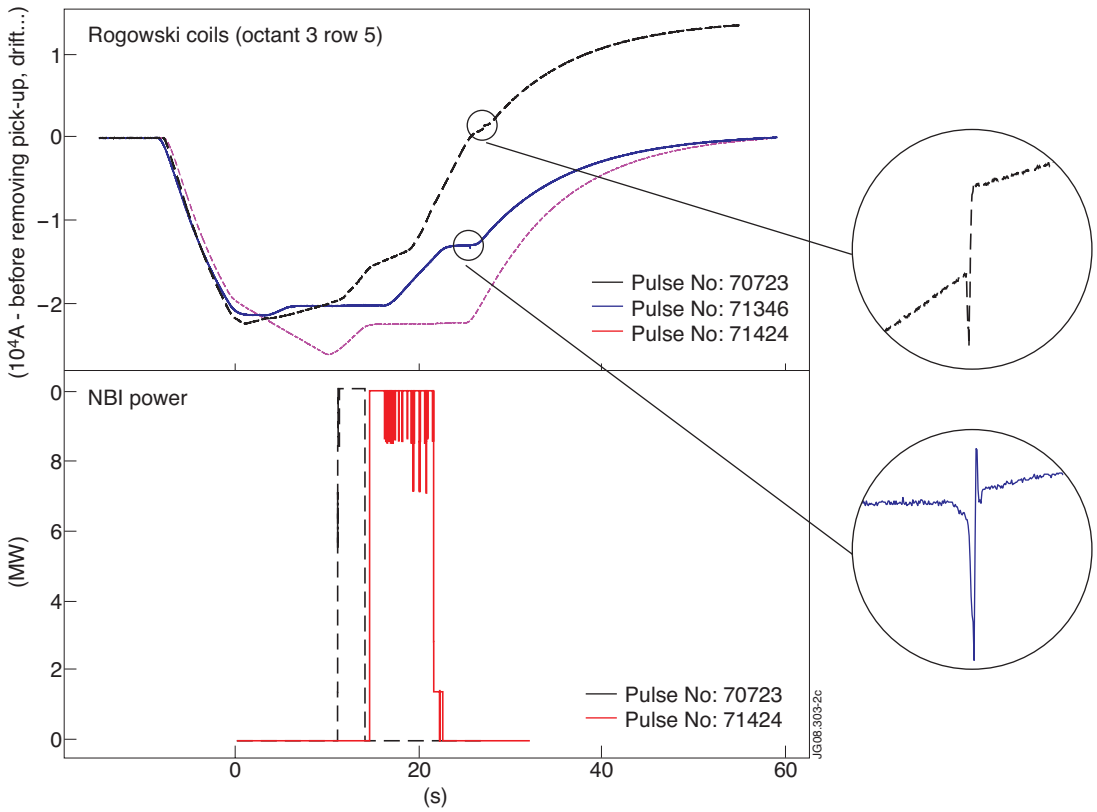

Figure 2: Raw signal of a Rogowskii coil before (Pulse No: 70723) and after (Pulse No's: 71346 and 71424) the 2007 repair which removed plasma and NB drift and step at the disruption.

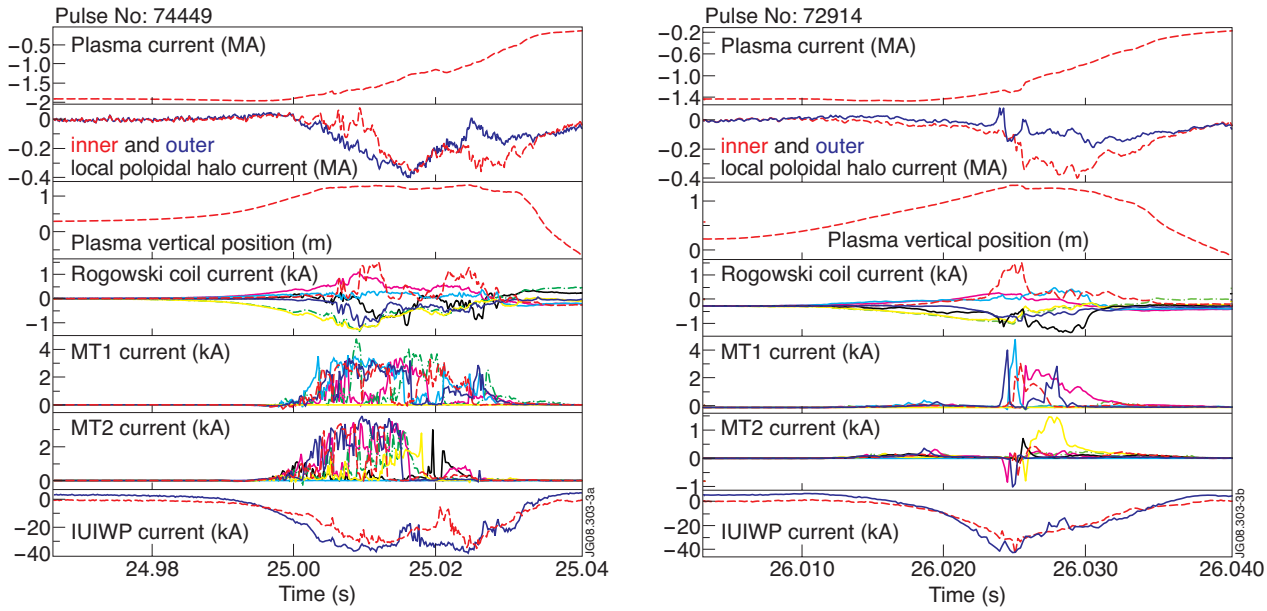

Figure 3: Overview of halo diagnostic observations for two typical ohmic vertical disruptions: (a) low triangularity - Pulse No: 74449 and (b) high triangularity - Pulse No: 72914.

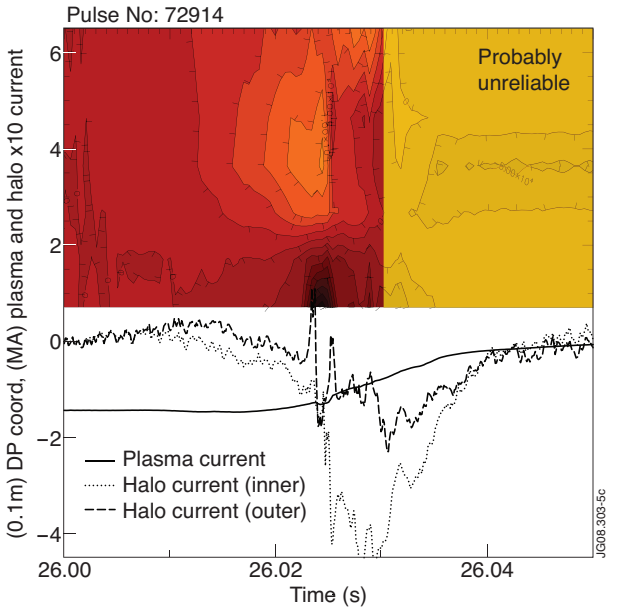

Figure 4: Collected halo current density on the dump plate at octant 3 during the VDE (vertical displacement event) of Pulse No: 72914 (ohmic, high triangularity), together with the plasma current and the poloidal halo current seen by the TF pick-up coils at the inner and outer edge of the dump plate at octant 3.

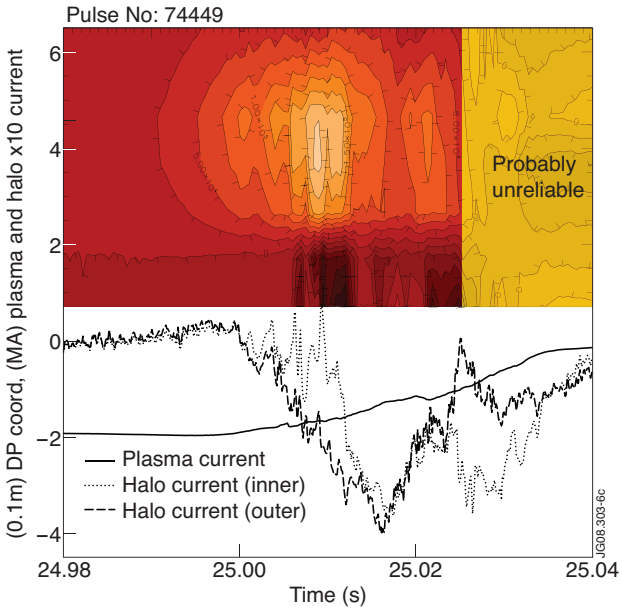

Figure 5: Collected halo current density on the dump plate at octant 3 during the disruption of Pulse No: 74449 (ohmic, low triangularity), together with the plasma current and the poloidal halo current seen by the TF pick-up coils at the inner and outer edge of the dump plate at octant 3.

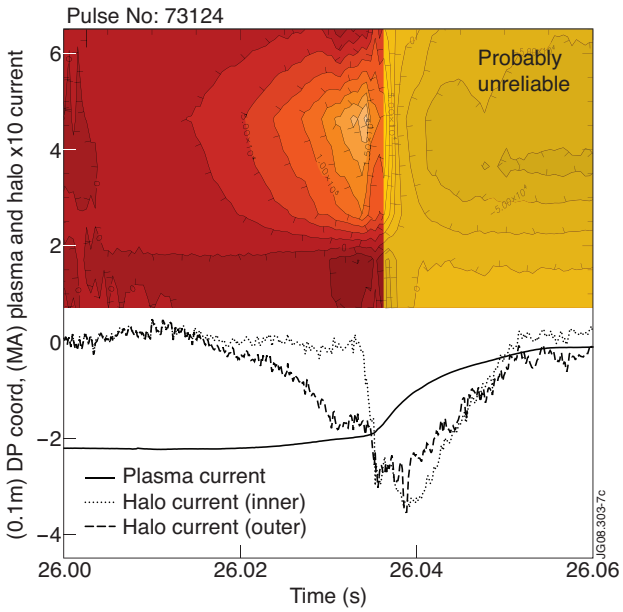

Figure 6: Collected halo current density on the dump plate at octant 3 during the VDE of Pulse No: 73124 (high energy, high triangularity), together with the plasma current and the poloidal halo current seen by the TF pick-up coils at the inner and outer edge of the dump plate at octant 3.

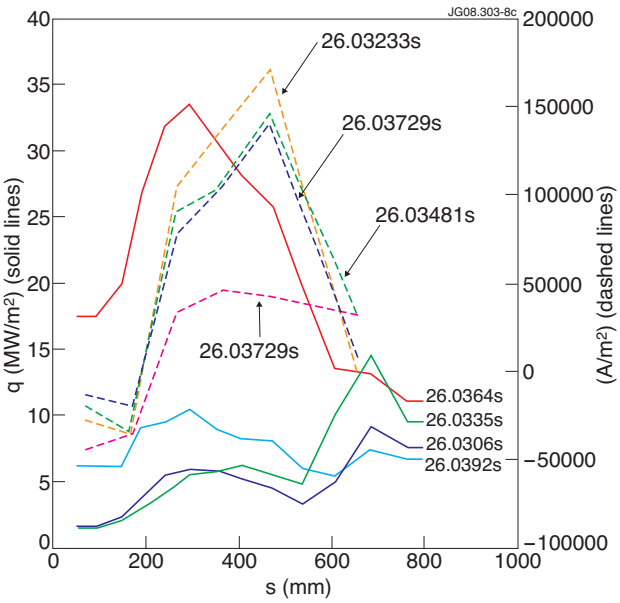

Figure 7: Power density (left axis) and halo current density (right axis) poloidal distribution for Pulse No: 73124 at times before and after the thermal quench.

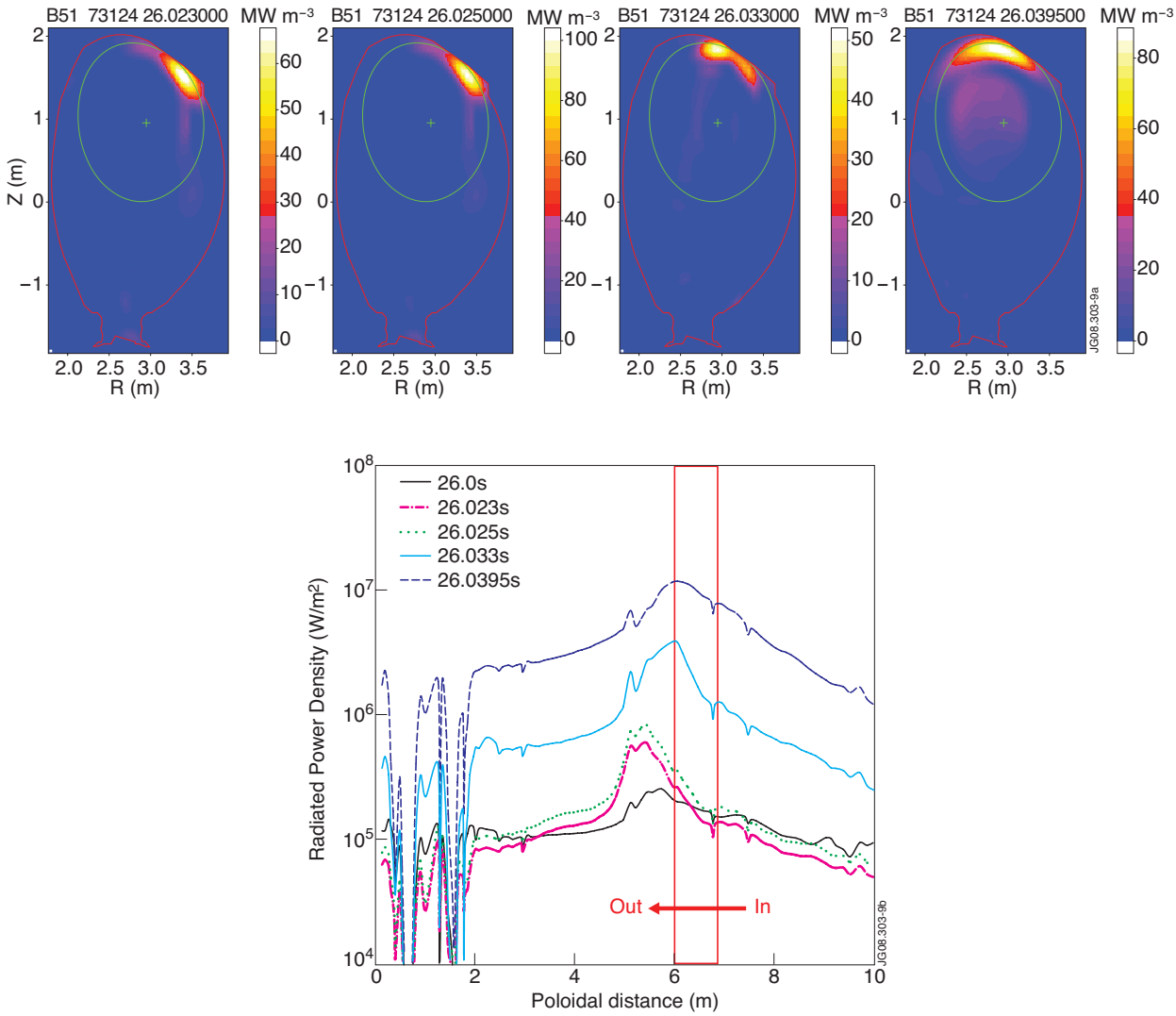

Figure 8: Top: tomographic reconstruction of the plasma radiation based and overlaid on the last converged EFIT equilibrium at the beginning and during the vertical displacement, at the thermal quench and at the total radiation peak for Pulse No: 73124. Bottom: radiation poloidal profiles at the same times as the tomographic reconstruction and before the vertical instability was initiated; here the dump plate is between 6.0 m (outer) and 6.8 m (inner).